

**KERNFORSCHUNGSZENTRUM**

**KARLSRUHE**

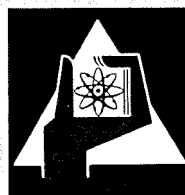
May 1970

KFK 1232

Institut für Angewandte Kernphysik

The Excited States of  $^{62}\text{Ni}$  Studied by the  $(n, \gamma)$  Reaction

U. Fanger, D. Heck, W. Michaelis, H. Ottmar, H. Schmidt, R. Gaeta



**GESELLSCHAFT FÜR KERNFORSCHUNG M. B. H.**

**KARLSRUHE**



## THE EXCITED STATES OF $^{62}\text{Ni}$ STUDIED BY THE $(n, \gamma)$ REACTION

U. FANGER, D. HECK, W. MICHAELIS, H. OTTMAR, H. SCHMIDT and R. GAETA †

*Institut für Angewandte Kernphysik  
Kernforschungszentrum Karlsruhe, Karlsruhe, Germany*

Received 19 January 1970

**Abstract:** The electromagnetic transition modes and level structure in  $^{62}\text{Ni}$  have been investigated via the radiative capture of thermal neutrons in  $^{61}\text{Ni}$ . Enriched samples of 92.11 %  $^{61}\text{Ni}$  were used as external targets in filtered reactor neutron beams. High-energy precision has been obtained by using Ge(Li) anti-Compton and Ge(Li) pair spectrometers. Coincidence relationships were found with a Ge(Li)-NaI(Tl) detector system, spin sequences and multipole mixing ratios have been deduced by measurements with a NaI-NaI angular correlation apparatus. The experimental data allow the construction of a considerably extended transition diagram up to 5 MeV with new spin and parity assignments for a large number of levels. The neutron separation energy of  $^{62}\text{Ni}$  was determined to be  $10596.2 \pm 1.5$  keV. Basing on intensities and  $\delta$ -values, ratios of reduced transition rates can be given in some cases. The experimental level scheme and transition branching ratios are compared with results of several shell-model calculations. The agreement of excitation energies is fairly good up to 3.2 MeV.

E NUCLEAR REACTIONS  $^{61}\text{Ni}(n, \gamma)$ ,  $E = \text{th}$ ; measured  $E_\gamma$ ,  $I_\gamma$ ,  $\gamma\gamma$ -coin,  $\gamma\gamma(\theta)$ ; deduced  $Q$ .  $^{62}\text{Ni}$  deduced levels,  $J$ ,  $\pi$ ,  $\delta$ ,  $\gamma$ -branching. Enriched target, Ge(Li) and NaI(Tl) detectors.

### 1. Introduction

In the past few years the nickel isotopes have been the subject of extensive experimental and theoretical studies. These nuclei in the vicinity of doubly-closed shells are considered to be spherical. In earlier macroscopic descriptions the low-lying excited states of the even nickel isotopes have been interpreted as surface oscillations<sup>1-3</sup>). Indeed, some regularities in the spectra and the strongly enhanced E2 transition strengths seem to support the collective point of view. On the other hand, attempts to understand the structure of these nuclei in the microscopic model were also successful. Besides quasiparticle and seniority approximations, recently exact shell-model calculations have been performed by Hsu<sup>4</sup>), Plastino *et al.*<sup>5</sup>), Cohen *et al.*<sup>6</sup>) and Auerbach<sup>7</sup>). In these calculations the authors assume an inert closed core of  $^{56}\text{Ni}$ , restrict the additional valence neutrons to the  $2p_{3/2}$ ,  $1f_{7/2}$  and  $2p_{1/2}$  orbits and hope to absorb the interactions with the core into effective residual interactions between the valence neutrons. Although the methods to determine the parameters of

† Visiting scientist from Junta de Energia Nuclear, Ciudad Universitaria, Madrid.

the effective interaction are different, almost equivalent fits for the experimental binding and level energies – used for the calculations – are obtained. A crucial check of the theories is not yet made, essentially due to a lack of experimental transition data.

This work is confined to the isotope  $^{62}\text{Ni}$ . A large number of levels in  $^{62}\text{Ni}$  up to an excitation energy of 8.5 MeV has been established by various reactions (stripping and pick-up reactions, Coulomb excitation, and inelastic scattering) and by  $\beta$ -decay studies<sup>8</sup>). Some of these investigations allow parity and also spin assignments. More recently both the  $\beta^-$  decay<sup>9</sup>) of  $^{62}\text{Co}$  ( $T_{1/2} = 13.9$  min,  $Q = 5.22$  MeV) and the  $\beta^+$  decay<sup>10</sup>) of  $^{62}\text{Cu}$  ( $T_{1/2} = 9.8$  min,  $Q = 3.94$  MeV) have been reinvestigated with Ge(Li) detectors. Newer information about the decay of  $^{62}\text{Ni}$  excited states found via the  $(p, p'\gamma)$  reaction has been given by Beuzit *et al.*<sup>11</sup>).

Nevertheless, further experimental data particularly concerning  $\gamma$ -transitions, spins, parities and branching ratios appear necessary for a detailed comparison with the theoretical predictions. Here the thermal neutron capture  $\gamma$ -ray method applying high-resolution Ge(Li) detector systems proves to be a valuable tool to obtain precise information up to high excitation energies. An investigation of this kind, the experimental equipment and procedure, the results and the deduced transition diagram will be described in the following sections. The  $^{61}\text{Ni}(n, \gamma)^{62}\text{Ni}$  reaction has not been studied before.

The data being discussed in this paper have been extracted from measurements performed in 1967. Preliminary results were given elsewhere<sup>12-14</sup>).

## 2. Experimental procedure

### 2.1. BEAM AND TARGET

Metallic Ni powder samples were used as external targets for thermalized neutrons at horizontal channels of the Karlsruhe research reactor FR 2. Bragg reflection or Bi crystal filtering was applied for monochromizing the reactor neutrons<sup>15</sup>). The neutron flux at the target positions was within  $3.5 \cdot 10^6 \text{ n} \cdot \text{cm}^{-2} \cdot \text{sec}^{-1}$  and  $1 \cdot 10^8 \text{ n} \cdot \text{cm}^{-2} \cdot \text{sec}^{-1}$  at a normal reactor power of 44 MW. The neutron tubes near the detectors consisted of double-walled cylinders filled with 7.5 mm  $^6\text{Li H}$  to protect the detectors against neutrons scattered from the samples and their 0.5 mm thin polythene containers.

The isotope  $^{61}\text{Ni}$  has a thermal neutron capture cross section of 2b and is represented only to 1.2% in the natural element, thus yielding a capture contribution of 0.6% (cf. table 1). For the samples used in these experiments the capture contribution had been increased to 83.5% by an enrichment in  $^{61}\text{Ni}$  to 92.11%. Impurities (i.e. other elements than nickel) have contributions of less than a few parts per thousand calculated with the best known  $\sigma$ -values and the abundances given by the manufacturer. One exception is the chemical contaminant Cd found by spectrographic analysis. When calculating the interference from the upper limit of 0.05% given for its abundance, one had to expect 67 captures in Cd per 100 captures in  $^{61}\text{Ni}$ . Fortu-

nately the contribution of Cd proved to be only 5% (due to the measured strength of the most intense line), which corresponds to an abundance of 0.004%.

## 2.2. APPARATUS

The  $\gamma$ -radiation following the capture of neutrons was detected with four devices: (i) an anti-Compton arrangement<sup>18)</sup> with a 4.9 cm<sup>3</sup> Ge(Li) diode for the low-energy portion up to 2.8 MeV, (ii) a 5-crystal pair spectrometer<sup>19)</sup> with a 2 mm  $\times$  2.7 cm<sup>2</sup> Ge(Li) detector, (iii) a 34 cm<sup>3</sup> Ge(Li) 7.6  $\times$  7.6 cm NaI(Tl) coincidence system<sup>20)</sup>, and (iv) an angular correlation spectrometer with two 10.2  $\times$  12.7 cm NaI(Tl) crystals<sup>21)</sup>. The latter two instruments were coupled to an on-line computer<sup>22)</sup>.

TABLE I  
Sample used for the  $^{61}\text{Ni}(n, \gamma)^{62}\text{Ni}$  investigation

Isotope	Binding energy <sup>a)</sup> of the neutron in the product nucleus (MeV)	Capture cross section <sup>b)</sup> for thermal neutrons (b)	Natural nickel		$^{61}\text{Ni}$ enriched sample	
			content (%)	capture contribution (%)	content (%)	capture contribution (%)
Ni	9.00	4.4	67.88	70	1.62	3
Ni	7.82	2.6	26.23	16	5.18	6
Ni	10.59	2.0	1.19	0.6	92.11	83.5
Ni	6.84	15	3.66	13	1.08	7.5
Ni	6.13	1.52	1.08	0.4	<0.05	<0.03

Ref. 16).      <sup>b)</sup> Ref. 17).

## 2.3. CALIBRATION

The energy calibration is based on the decay lines of  $^{57}\text{Co}$ ,  $^{88}\text{Y}$  [ref. 23)],  $^{137}\text{Cs}$  [ref. 24)],  $^{192}\text{Ir}$ ,  $^{60}\text{Co}$  [ref. 25)] and capture  $\gamma$ -rays of the reaction  $\text{H}(n, \gamma)$  [ref. 26)] up to 2.8 MeV and on capture lines in  $^{56}\text{Fe}$  [ref. 27)],  $^{164}\text{Dy}$  [ref. 28)] and  $^{14}\text{N}$  [ref. 29)] in the higher-energy region.

The response function of the anti-Compton spectrometer was known from measurements with absolutely calibrated radioactive sources. For the pair spectrometer the response function was determined by measuring the capture  $\gamma$ -ray spectrum from natural nickel; the intensities of these  $\gamma$ -lines were given in quanta per 100 captures by Groshev *et al.*<sup>16)</sup>. One of the natural nickel lines (a very weak one) originates from  $^{62}\text{Ni}$ . Vice versa, the strongest lines of  $^{61}\text{Ni}$  and  $^{63}\text{Ni}$  produce pronounced peaks in the  $^{62}\text{Ni}$  spectrum (see fig. 1). Thus, considering the capture contributions one can easily calculate the  $^{62}\text{Ni}$  line intensities in quanta per 100 captures in  $^{61}\text{Ni}$ . All the  $\gamma$ -ray spectra have been analysed by a fit program using modified Gaussian func-

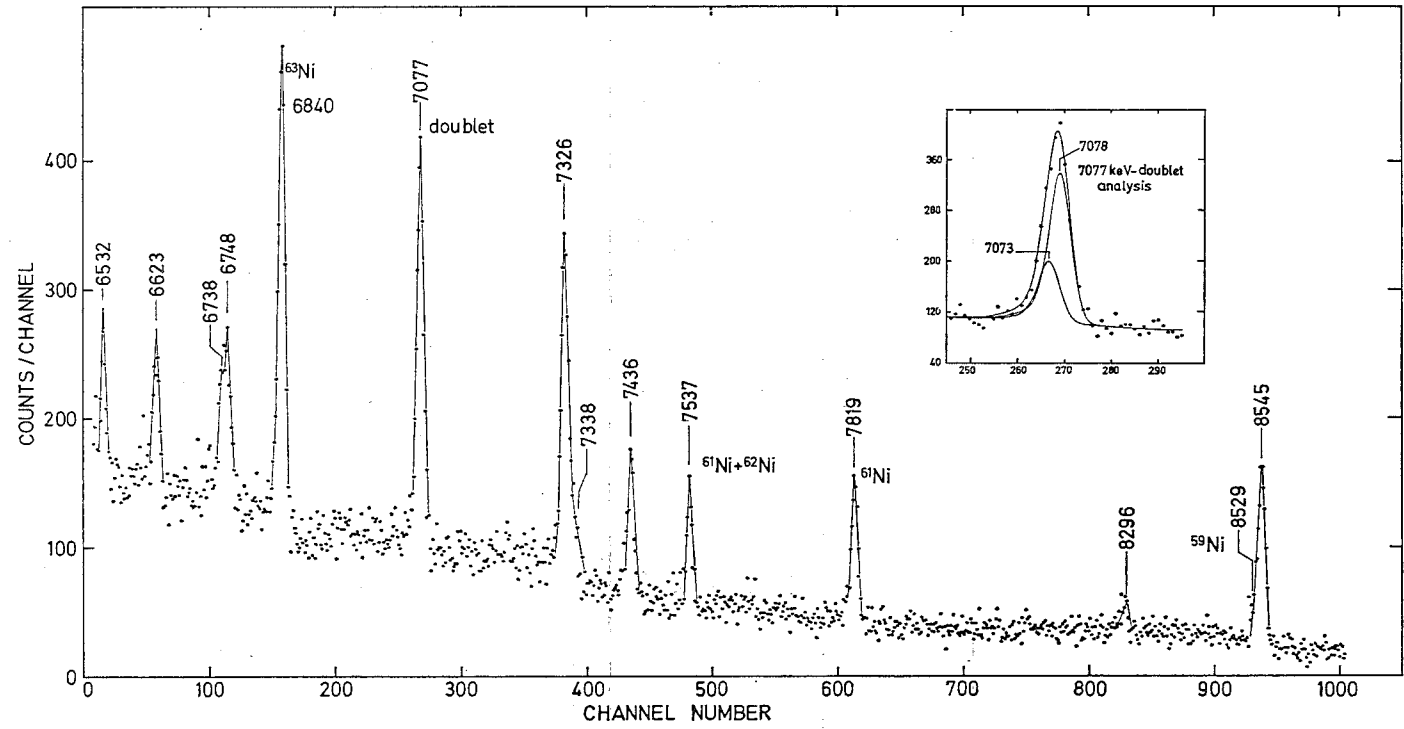


Fig. 1. Portion of the capture spectrum from the  $^{61}\text{Ni}$  enriched sample as observed with the pair spectrometer. The inset displays the computer analysis of the 7077 keV doublet.

tions<sup>30</sup>). It determines the peak positions, calculates the energies by a least-squares-fit polynomial of the 4th order, and yields efficiency-corrected intensities.

#### 2.4. EVALUATION OF THE ANGULAR CORRELATION MEASUREMENTS

The NaI-NaI coincidence spectra observed at the different angles were processed on an off-line computer as described in ref.<sup>21</sup>). The intensity analysis of complex peak structures in the NaI spectra was done, too, by the just mentioned Gaussian fit program. As a measure of the intensities of the  $\gamma$ -transitions the total absorption peak areas were used assuming standard line shapes. An important factor in the analysis was the knowledge of the  $\gamma$ -ray energies and their relative intensities obtained from the Ge(Li) data. The coefficients appropriate to the usual Legendre polynomial expansion for the correlation function  $W(\vartheta) = 1 + A_2P_2(\cos \vartheta) + A_4P_4(\cos \vartheta)$  were computed from the coincidence intensities applying the method of least squares. Corrections for the finite size of the source and the detectors and due to the interaction processes of the  $\gamma$ -quanta in the source were taken into account<sup>31</sup>).

### 3. Experimental results

#### 3.1. ENERGIES AND INTENSITIES OF NEUTRON CAPTURE $\gamma$ -LINES IN $^{62}\text{Ni}$

As an example for the  $\gamma$ -ray spectra taken with the pair spectrometer the portion from 6.4 to 8.6 MeV is shown in fig. 1. As expected from the 16.5% capture contribution of isotopes other than  $^{61}\text{Ni}$ , strong lines of  $^{59}\text{Ni}$ ,  $^{61}\text{Ni}$  and  $^{63}\text{Ni}$  also do appear. An interesting point in the later interpretation of the level scheme is the computer analysis of the 7077 keV doublet. The energy difference of the doublet lines is 5 keV. Tables 2 and 3 are compilations of the energies and intensities of  $\gamma$ -rays which have been observed in the  $^{61}\text{Ni}(n, \gamma)^{62}\text{Ni}$  investigation. The given uncertainties in the energy values contain statistical errors, systematical fit errors, and the errors of the calibration energies taken from the literature. The intensities are normalized to correspond to quanta per 100 captures in  $^{61}\text{Ni}$  (cf. subsect. 2.3). The uncertainties of the intensities include errors in the line fit and the adaptation of the response functions and statistical errors. Due to the indirect method of the absolute intensity determination, one has to consider, too, errors in the capture contributions (i.e. isotopic cross sections) and errors in the intensities of  $^{59, 61, 63}\text{Ni}$  lines taken from the literature. The systematic intensity errors are believed to sum up to 10%-20%, dependent on the energy range. The absolute intensity scale is fixed at lines between 6.8 and 9.4 MeV. In the column headed by "assignment" the  $^{62}\text{Ni}$  transitions are indicated by arrows between level energy values (given in keV). Some of the background lines could be identified as originating from  $(n, \gamma)$  reactions or  $\beta$ -decay.

#### 3.2. GAMMA-GAMMA COINCIDENCES

Sections of two of the Ge(Li) spectra as obtained by using the double window coincidence technique are shown in fig. 2. The spectra are coincident with NaI

TABLE 2

Gamma rays in the energy range from 150 keV to 2800 keV, measured with the anti-Compton spectrometer

$E_\gamma$ (keV)	$\pm \Delta E_\gamma$ (eV)	$I_\gamma$	$\pm \Delta I_\gamma$	Assignment
155.46	80	(1.7)	0.2	$^{62}\text{Ni}(n, \gamma)$
169.4	500	0.04	0.02	
179.1	600	0.04	0.02	
185.54	450	0.05	0.02	
188.67	460	0.05	0.02	
195.1	650	0.04	0.02	
213.33	360	0.06	0.02	bg (?)
232.6	500	0.02	0.01	
237.75	400	0.03	0.01	
244.54	150	0.20	0.03	
247.79	250	0.08	0.02	
264.94	250	0.10	0.02	3522.69 $\rightarrow$ 3257.00
282.92	100	(2.8)	0.3	$^{60}\text{Ni}(n, \gamma)$
295.6	550	0.07	0.04	
310.36	450	0.09	0.04	4628 $\rightarrow$ 4318
314.3	600	0.07	0.04	
326.5	500	0.08	0.04	
331.4	800	0.05	0.03	
339.47	200	0.30	0.05	
362.09	130	(0.60)	0.08	$^{62}\text{Ni}(n, \gamma)$
379.8	500	0.06	0.03	bg (?)
450.4	700	0.04	0.02	3972.20 $\rightarrow$ 3522.69
459.74	250	0.35	0.05	3518.52 $\rightarrow$ 3058.63
464.63	150	1.5	0.2	3522.69 $\rightarrow$ 3058.63
479.6	1000	0.4	0.3	3370.0 $\rightarrow$ 2891.06
524.63	400	0.20	0.06	
534.3	600	0.14	0.05	
558.42	120	(1.8)	0.2	$^{113}\text{Cd}(n, \gamma)$
568.5	500	0.17	0.10	
575.65	450	0.20	0.07	
579.42	200	0.55	0.06	3849.31 $\rightarrow$ 3269.72
590.82	450	0.20	0.05	
650.03	450	(0.30)	0.08	$^{113}\text{Cd}(n, \gamma)$
654.9	500	0.30	0.08	
675.16	450	0.36	0.10	
678.50	300	0.55	0.15	4201 $\rightarrow$ 3522.69
695.4	700	0.30	0.10	
703.1	600	0.20	0.08	3972.20 $\rightarrow$ 3269.72
722.0	500	0.65	0.20	3058.63 $\rightarrow$ 2336.10
756.76	300	1.55	0.25	3058.63 $\rightarrow$ 2301.46
845.91	450	(0.50)	0.20	$^{62}\text{Ni}(n, \gamma)$
855.6	500	0.55	0.20	3157.65 $\rightarrow$ 2301.46
875.64	80	14.3	1.5	2048.44 $\rightarrow$ 1172.80
968.16	400	0.52	0.15	3269.72 $\rightarrow$ 2301.46 (3860.0 $\rightarrow$ 2891.06?)
1045.90	350	0.50	0.10	4416 $\rightarrow$ 3370.0
1067.6	800	0.35	0.10	3370.0 $\rightarrow$ 2301.46

TABLE 2 (continued)

$E_\gamma$ (keV)	$\pm\Delta E_\gamma$ (eV)	$I_\gamma$	$\pm\Delta I_\gamma$	Assignment
1092.50	250	0.9	0.2	4151.4 → 3058.63
1128.73	100	6.8	0.8	2301.46 → 1172.80
1163.30	150	5.8	1.1	2336.10 → 1172.80
1172.80	100	75.7	4.0	1172.80 → 0
1185.85	380	2.5	0.4	3522.69 → 2336.10
1220.76	350	5.2	0.7	3269.72 → 2048.44 3522.69 → 2301.46
1322.1	600	0.30	0.10	3370.0 → 2048.44
1455.2	500	0.40	0.10	3756.6 → 2301.46
1470.4	450	0.45	0.10	3518.52 → 2048.44
1538.6	750	0.30	0.15	
1548.02	480	0.5	0.2	3849.31 → 2301.46
1661.3	700	0.4	0.2	4719 → 3058.63
1718.26	250	1.2	0.3	2891.06 → 1172.80
1760.97	450	1.0	0.2	4062.4 → 2301.46
1815.8	800	0.4	0.2	4151.4 → 2336.10
1850.0	700	0.6	0.2	4151.4 → 2301.46
1886.23	350	1.7	0.4	3058.63 → 1172.80
1985.13	280	4.1	0.6	3157.65 → 1172.80
2034.4	700	0.7	0.3	
2048.7	1000	0.5	0.2	
2084.20	300	4.0	0.6	3257.00 → 1172.80
2097.32	300	7.2	1.2	3269.72 → 1172.80
2104.7	700	0.9	0.3	
2123.6	600	(0.9)	0.3	$^{60}\text{Ni}(n, \gamma)$
2155.8	800	0.5	0.2	
2188.5	1500	0.23	0.15	
2196.5	800	0.4	0.2	
2289.7	1500	0.28	0.15	4628 → 2336.10
2301.41	120	10.4	1.5	2301.46 → 0
2345.64	200	4.5	0.9	3518.52 → 1172.80
2583.6	1200	0.5	0.3	3756.6 → 1172.80
2799.40	450	1.8	0.7	3972.20 → 1172.80

Reaction:  $^{61}\text{Ni}(n_{\text{th}}, \gamma)^{62}\text{Ni}$ . Target: Metallic nickel powder enriched to 92.11 % in  $^{61}\text{Ni}$ . The intensities are normalized to  $100 \pm 20$  captures in  $^{61}\text{Ni}$  (cf. text).

windows around the lines at 876 keV (lower spectrum) and 1173 keV (upper spectrum). The window positions in the NaI spectrum are indicated in the inset. The window on the complex peak at 1173 keV contains five lines.

The results of the coincidence measurements are summarized in the tables 4, 5, 6. The coincidence relationships have been found analysing the data by the window subtraction method as well as by comparison of spectra. The two modes of coincidence measurements with the Ge(Li)-NaI system, namely window setting in the NaI spectrum (table 4) or in the Ge(Li) spectrum (table 5) yield a useful redundancy or give complementary information in the case of complex peak structures. In table 6

TABLE 3

Gamma lines in the energy range from 2.9 MeV to 10.6 MeV

$E_\gamma$ (keV)	$\pm\Delta E_\gamma$ (keV)	$I_\gamma$	$\pm\Delta I_\gamma$	Assignment
2950	2	0.55	0.2	
2961	2	0.6	0.2	
2972	1.5	1.05	0.2	
2984	2	0.65	0.2	
3001	2	0.55	0.3	$^{113}\text{Cd}(n, \gamma)$ (?)
3032	3	0.35	0.2	
3060	2	0.5	0.1	3058.63 $\rightarrow$ 0
3095	2	0.6	0.1	
3158	1.5	1.7	0.2	3157.65 $\rightarrow$ 0
3175	2	0.3	0.1	
3207	2	0.4	0.1	
3270	1	1.6	0.2	3269.72 $\rightarrow$ 0
3295	1.5	0.6	0.1	
3370	2	1.55	0.4	3370.0 $\rightarrow$ 0
3443	2	0.4	0.1	
3456	3	0.35	0.1	4628 $\rightarrow$ 1172.80
3474	3	0.25	0.1	
3518	3	0.3	0.1	3518.52 $\rightarrow$ 0
3546	2	0.35	0.1	4719 $\rightarrow$ 1172.80
3812	2	0.55	0.1	
3828	2	0.55	0.1	4999 $\rightarrow$ 1172.80
3860	1.5	1.6	0.2	3860.0 $\rightarrow$ 0
3880	2	0.4	0.1	
3963	4	0.15	0.1	
3972	1.5	1.2	0.2	3972.20 $\rightarrow$ 0
3981	3	0.5	0.1	
3990	2	0.45	0.1	
4035	2	0.6	0.1	
4043	3	0.25	0.1	
4061	2	0.9	0.1	4062.4 $\rightarrow$ 0
4127	2	0.45	0.1	
4318	3	0.25	0.1	4318 $\rightarrow$ 0
4341	2	0.35	0.1	
4379	2	0.3	0.1	
4416	2	0.4	0.1	4416 $\rightarrow$ 0
4424	2	0.35	0.1	
4482	2	(0.25)	0.1	$^{61}\text{Ni}(n, \gamma) + ^{62}\text{Ni}(n, \gamma)$ (?)
4566	2	0.2	0.1	
4713	2	0.25	0.1	
4731	3	0.15	0.1	
4850	1.5	0.5	0.1	
4880	3	0.25	0.1	
4945	3	0.35	0.1	$^{12}\text{C}(n, \gamma)$ (?)
4998	2	0.45	0.1	4999 $\rightarrow$ 0
5018	2	0.3	0.1	
5037	2	0.45	0.1	
5052	3	0.15	0.1	
5074	3	0.15	0.1	

TABLE 3. (continued)

$E_\gamma$ (keV)	$\pm \Delta E_\gamma$ (keV)	$I_\gamma$	$\pm \Delta I_\gamma$	Assignment
5162	1.5	0.5	0.1	
5292	1.5	0.8	0.1	
5300	3	0.15	0.1	
5354	2	0.25	0.1	
5386	1.5	0.5	0.1	
5428	3	0.15	0.1	$^{113}\text{Cd}(n, \gamma)$ (?)
5440	3	0.2	0.1	
5517	2	(0.25)	0.1	$^{62}\text{Ni}(n, \gamma)$
5539	2	0.4	0.1	
5570	2	0.2	0.1	
5596	4	0.15	0.1	C $\rightarrow$ 4999
5607	2	0.35	0.1	
5695	2	(0.3)	0.1	$^{60}\text{Ni}(n, \gamma)$
5820	2	0.25	0.1	$^{113}\text{Cd}(n, \gamma)$ (?)
5834	2	(0.35)	0.1	$^{62}\text{Ni}(n, \gamma)$
5877	2	0.3	0.1	C $\rightarrow$ 4719
5968	2	0.7	0.1	C $\rightarrow$ 4628
6018	3	0.25	0.1	
6035	3	0.2	0.1	
6087	3	0.25	0.1	
6111	4	0.2	0.1	$^{35}\text{Cl}(n, \gamma)$ (?)
6179	2	1.0	0.2	C $\rightarrow$ 4416
6277	3	0.4	0.2	C $\rightarrow$ 4318
6321	2	(0.4)	0.2	$^{62}\text{Ni}(n, \gamma)$
6364	2	0.5	0.3	C $\rightarrow$ 4232
6387	2	0.4	0.2	C $\rightarrow$ 4209
6395	2	0.5	0.3	C $\rightarrow$ 4201
6445	2	1.2	0.2	C $\rightarrow$ 4151.4
6532	2	1.8	0.4	C $\rightarrow$ 4062.4
6623	2	1.7	0.3	C $\rightarrow$ 3972.20
6738	3	1.2	0.2	C $\rightarrow$ 3860.0
6748	3	1.3	0.2	C $\rightarrow$ 3849.31
6840	1.5	(5.9)	0.4	$^{62}\text{Ni}(n, \gamma)$ ; C $\rightarrow$ 3756.6 (?)
7073	3	1.5	0.7	C $\rightarrow$ 3522.69
7078	1.5	3.6	0.7	C $\rightarrow$ 3518.52
7326	1.5	4.8	0.4	C $\rightarrow$ 3269.72
7338	2	1.4	0.3	C $\rightarrow$ 3257.00
7436	2	2.0	0.3	C $\rightarrow$ 3157.65
7537	2	(1.7)	0.3	$^{60}\text{Ni}(n, \gamma)$ ; C $\rightarrow$ 3058.63
7819	2	(2.5)	0.3	$^{60}\text{Ni}(n, \gamma)$
8296	3	0.8	0.2	C $\rightarrow$ 2301.46
8529	4	(0.6)	0.3	$^{58}\text{Ni}(n, \gamma)$
8545	3	4.6	0.5	C $\rightarrow$ 2048.44
8998	3	(1.3)	0.4	$^{58}\text{Ni}(n, \gamma)$
9425	3	5.0	0.5	C $\rightarrow$ 1172.80
10597	3	3.7	0.8	C $\rightarrow$ 0

Reaction:  $^{61}\text{Ni}(n_{th}, \gamma)^{62}\text{Ni}$ . Target: Metallic nickel powder enriched to 92.11 % in  $^{61}\text{Ni}$ . The intensities are normalized to  $100 \pm 20$  captures in  $^{61}\text{Ni}$  (cf. text).

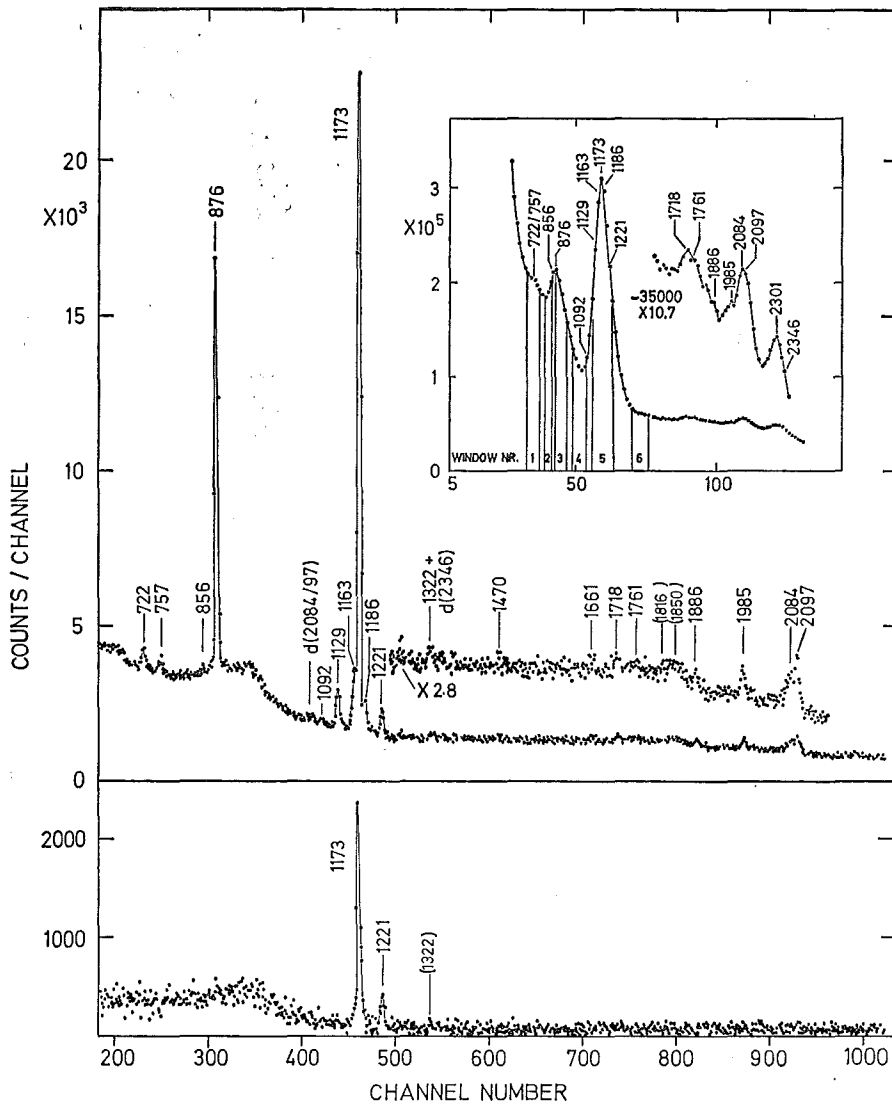


Fig. 2. Two Ge(Li) spectra in coincidence with  $\gamma$ -lines observed with a NaI(Tl) detector. The window positions in the NaI spectrum are indicated in the inset. The lower and upper spectrum are coincident with lines at 876 keV and 1173 keV, respectively, and have been obtained by means of the window subtraction method.

the results of two types of measurements are comprised: normal and sum coincidences observed with two NaI detectors. The electronic sum window was set at a  $\gamma$ -ray pulse height corresponding to the binding energy of the last neutron. The low-energy coincidences have been partly omitted in table 6.

TABLE 4  
NaI(Tl)-Ge(Li) coincidences of  $^{62}\text{Ni}$   $\gamma$ -rays

Window NaI (MeV)	Main lines (keV) in window	Coincident lines (keV) in Ge(Li) spectrum	Interpretation (cascades) (keV)
0.47-0.55	480, 525, 534	1173; 1718	480-1718-1173
0.79-0.87	856	1129; 1173; 2301	856-1129-1173; 856-2301
0.87-0.96	876	1173; 1221; 1322; 1470	876-1173, 1221, 1322, 1470
0.98-1.09	1046, 1068, 1092	(757) <sup>a</sup> ; 1129; 1173; 2301	1068-2301; 1068-1129-1173; (1092-757)
1.11-1.25	1129, 1163, 1173, 1186, 1221	579; 722; 757; (856); 876; 1092; 1129; (1163); 1173; 1186; 1221; 1322; 1470; 1718; 1886; 1985; 2084; 2097; 2346; 2799; (2984); (3032); (3880); (4713)	1173-876, 1129, (1163), 1718, 1886, 1985, 2084, 2097, 2346, 2799, 3880, 4713; 1173-876-1221, 1322, 1470; 1129-856; 1129-757-1092; 1163-722, 1186
1.83-1.93	1850, 1886	465; 1092; 1173	1886-465, 1092, 1173
1.95-2.03	1985	1173	1985-1173
2.03-2.14	2034, 2049, 2084, 2097	579	2097-579
2.25-2.34	2290, 2301, s.e. 2799	757; 1173; 1221; (1661)	2301-757(-1661); 2301-1221* <sup>b</sup> ; 2799-1173
2.34-2.43	2346	1173	2346-1173

Energy range:  $0 < E_\gamma < 4.3$  MeV. Windows set in the NaI spectrum.

<sup>a</sup>) Weak coincident lines are given in brackets.

<sup>b</sup>) Evidently a second 1221 keV transition.

TABLE 5  
NaI(Tl)-Ge(Li) coincidences of  $^{62}\text{Ni}$   $\gamma$ -rays

Window Ge(Li); lines (keV)	Coincident lines (keV) in NaI spectrum	Interpretation (cascades) (keV)
480	1718; 1173	480-1718-1173
722	1173	722(-1163)-1173
757	1173; 2301	757-2301; 757(-1129)-1173
876	1173; 1470	876-1173, 1470
1129	757; 1173; 1455; (1548) <sup>a</sup> ; (1661)	1129-757(-1661); 1129-1173, 1455, (1548)
1173	... <sup>b</sup> ; 2084/2097; 2346	1173-2084, 2097, 2346
1221	876; 1173; 2301	1221-876-1173; 1221*-2301
1985	3295	
2301	856; 1221; 1761	2301-856, 1221*, 1761

Energy range:  $0 < E_\gamma < 4.3$  MeV. Windows set in the Ge(Li) spectrum.

<sup>a</sup>) Weak coincident lines in brackets.

<sup>b</sup>) Range up to 2 MeV could not be evaluated.

TABLE 6  
NaI-NaI coincidences of  $^{62}\text{Ni}$   $\gamma$ -rays

6a) Two-step cascades <sup>a</sup> ) (MeV) observed in the sum-coincidence spectrum. Gate at the binding energy 10.6 MeV									
9.42	8.30	7.33	7.08	6.74	6.62	6.53	6.18	5.60	
1.17	2.30	3.27	3.52	3.86	3.97	4.06	4.42	5.00	
6b) Coincidence relationships resulting from measurements with different gates									
Window at line <sup>b</sup> ) (MeV)	Prominent lines (MeV) in coincidence					Interpretation (cascades) (keV)			
7.44	2.30; 1.98; 1.17					7436-1985-1173; 7436-(856-)2301			
7.33	3.27; 2.10; 1.17; 0.88					7326-3270; 7326-2097-1173; 7326-(1220-) 875			
7.08	2.33; 1.89; 1.47; 1.17; 0.88; 0.76					7078-2346; 7073-(1221*-)2301; 7078-(465-)1886; 7078-1470-876-1173; 7078-(465-)757			
6.62, 6.53	4.06; 3.97; 2.80; 1.76; 1.17					6532-4059; 6623-3972; 6623-2799-1173; 6532-1761			
2.30	2.20; 1.85; 1.76; (1.55) <sup>c</sup> ; 1.22					2301-1850; 2301-1761; (2301-1548); 2301-1221*			
1.17	9.42; 8.54; 8.30; (7.44); 7.33; 7.08; 6.62; ...					9425-1173; 8545-(876-)1173; 8296-(1129-) 1173; (7436-(1985-)1173); 7326-(2097-)1173; 7078-(2346-)1173; 6623-(2799-)1173; ...			
0.87	854; 7.44; ...					8545-876; 7436-856; ...			

<sup>a</sup>) Only prominent cascades are given in the table.

<sup>b</sup>) Coincidences with single- or double-escape peaks in the windows are excluded



### 3.3. LEVEL SCHEME

The results of these measurements on the reaction  ${}^{61}\text{Ni}(n, \gamma){}^{62}\text{Ni}$  suggest a level scheme as presented in fig. 3. It is based essentially on coincidence relationships, indicated in the diagram by full or open circles (for well established or probable coincidences, respectively). The energy combination principle was used with discretion and generally not thought a sufficient argument for the existence of a level. Possible states with excitation energies higher than 5 MeV, therefore, were not taken into consideration in this level scheme. The intensities of the transitions are expressed by the line widths. Two transitions are labelled with asterisks which serve to distinguish  $\gamma$ -lines that have been placed twice in the scheme. The position of one of these transitions marked by a dashed line is believed to be less certain.

The level spins have been determined by  $\gamma$ - $\gamma$  angular correlation measurements being discussed in the next subsect. (3.4). The spins of the ground state and the first four excited states were already well known. For a great part of levels the possible spins can be restricted according to the character of feeding and deexcitation. Strong primary transitions, for instance, which presumably have E1 character determine a positive level parity and the spins  $J = 0, 1, 2, 3$ , since the capturing state is an unknown  $\dagger$  mixture of  $1^-$  and  $2^-$  states. A good example for a unique spin parity determination from transitions is the level at 3059 keV: it is directly fed from the capture state ( $J = 0, 1, 2, 3$ ) and depopulated by transitions to the  $0^+$  ground state ( $J = 1, 2$ ) and to a  $4^+$  excited state ( $J^\pi = 2^+$ ). The neutron orbital momenta known from (d, p) reaction measurements have been used, too, for the parity determination of some of the levels.

The properties of the  ${}^{62}\text{Ni}$  levels observed in the (n,  $\gamma$ ) reaction i.e. spins and parities, feeding and deexcitation, and the  $\gamma$ -branching ratios are compiled in table 7. For a detailed comparison with other experimental level data we refer to the comprehensive collection in ref. <sup>8)</sup> or to the recent (p, p' $\gamma$ ) work <sup>11)</sup>.

### 3.4. LEVEL SPINS

Figs. 4a-c show some typical coincidence spectra relevant to the angular correlation measurements. The spectra are taken with the NaI(Tl) scintillation detector at  $90^\circ$  and at  $180^\circ$ . In order to make the figure clearer the  $180^\circ$  spectra are shifted upwards by a suitable amount. The coincident background is subtracted in each spectrum by application of the double window technique. A singles spectrum taken with the stationary detector is shown in fig. 4d. The photo-peak positions of the prominent  $\gamma$ -rays and their relative intensities are indicated in the figure by the position and length of vertical bars on the abscissa, together with the gate positions selected for the angular correlation measurements.

It is clear from an inspection of the figures that most of the peaks to be observed are complex. Unfortunately the Ge(Li) singles spectrum and the decay scheme were

<sup>†</sup> The spins of the lowest neutron resonances in  ${}^{61}\text{Ni}$  ( $J_g^\pi = \frac{3}{2}^-$ ) are unknown.

TABLE 7  
Properties of the <sup>62</sup>Ni excited states observed in the (n,  $\gamma$ ) reaction

No.	Level <i>E</i> (keV)	<i>J<math>\pi</math></i>	<i>I<math>\gamma</math></i> of direct feeding %	<i>I<math>\gamma</math></i> of total feeding %	<i>I<math>\gamma</math></i> of total deexcit- ation %	Transitions to level no.	$\gamma$ -branching ratios
0	0	0 <sup>+</sup>	3.7 (8)	100.2			
1	1172.80 (10)	2 <sup>+</sup>	5.0 (5)	58.1	75.7	0	
2	2048.44 (18)	0 <sup>+</sup>	4.6 (5)	7.5	14.3	1	
3	2301.46 (12)	2 <sup>+</sup>	0.8 (2)	9.4	17.2	0, 1	60 : 40
4	2336.10 (28)	4 <sup>+</sup>		3.8	5.8	1	
5	2891.06 (35)	2 <sup>+</sup>		0.4	1.2	1	
6	3058.63 (42)	2 <sup>+</sup>	0.2 (1)	3.3	4.4	0, 1, 3, 4	11 : 39 : 35 : 15
7	3157.65 (35)	2 <sup>+</sup>	2.0 (3)	2.0	6.3	0, 1, 3	27 : 65 : 8
8	3257.00 (40)	1 <sup>+</sup> , 2 <sup>+</sup> , 3 <sup>+</sup>	1.4 (3)	1.5	4.0	1	
9	3269.72 (40)	1 <sup>+</sup> , 2 <sup>+</sup>	4.8 (4)	5.5	11.4	0, 1, 2, 3	14 : 63 : 18 : 5
10	3370.0 (8)	1 <sup>+</sup> , 2 <sup>+</sup>		0.5	2.6	0, 2, 3, 5	60 : 12 : 13 : 15
11	3518.52 (30)	2 <sup>+</sup>	3.6 (7)	3.6	5.6	0, 1, 2, 6	5 : 80 : 8 : 6
12	3522.69 (50)	2 <sup>+</sup> , 3 <sup>+</sup>	1.5 (7)	2.1	7.2	3, 4, 6, 8	43 : 35 : 21 : 1
13	3756.6 (5)	3 <sup>-</sup>	<0.6	<0.6	0.9	1, 3	55 : 45
14	3849.31 (45)		1.3 (2)	1.3	1.1	3, 9	50 : 50
15	3860.0 (15)	1 <sup>+</sup> , 2 <sup>+</sup>	1.2 (2)	1.2	1.6	0, (5)	
16	3972.20 (55)	2 <sup>+</sup>	1.7 (3)	1.7	3.2	0, 1, 9, 12	37 : 55 : 6 : 1
17	4062.4 (6)	1 <sup>+</sup> , 2 <sup>+</sup>	1.8 (4)	1.8	1.9	0, 3	48 : 52
18	4151.4 (5)	2 <sup>+</sup> , 3 <sup>+</sup>	1.2 (2)	1.2	1.9	3, 4, 6	32 : 21 : 47
19	4201 (2)		0.5 (3)	0.5	0.5	12	
20	4209 (2)		0.4 (2)	0.4			
21	4232 (3)		0.5 (3)	0.5			
22	4318 (2)	1 <sup>+</sup> , 2 <sup>+</sup>	0.4 (2)	0.5	0.3	0	
23	4416 (2)	1 <sup>+</sup> , 2 <sup>+</sup>	1.0 (2)	1.0	0.9	0, 10	45 : 55
24	4628 (2)	2, 3	0.7 (1)	0.7	0.7	1, 4, 22	49 : 39 : 12
25	4719 (2)		0.3 (1)	0.3	0.8	1, 6	47 : 53
26	4999 (2)	1, 2	0.15(10)	0.15	1.0	0, 1	45 : 55
C	10596.2 (15)	1 <sup>-</sup> , 2 <sup>-</sup>			39.3	see coll. 4	see coll. 4

not known when we started with the angular correlation measurements<sup>†</sup>; thus in some cases the gates were not in the optimum position. In addition, it turned out that (because of the complexity of the gate spectrum) the number of windows used was too small. The spectral decomposition of a complex group containing lines of comparable intensities with energy differences less than about 50 keV was impossible even with the computer program. Therefore, the angular correlations observed are mostly sums of the individual correlations of the contributing cascades. In favourable cases information on the spins of the levels involved and on the multipolarities of the transitions can be obtained from consideration of the relative intensities and the

<sup>†</sup> Due to the limited time the enriched sample was available for this investigation the various measurements had to be performed simultaneously.

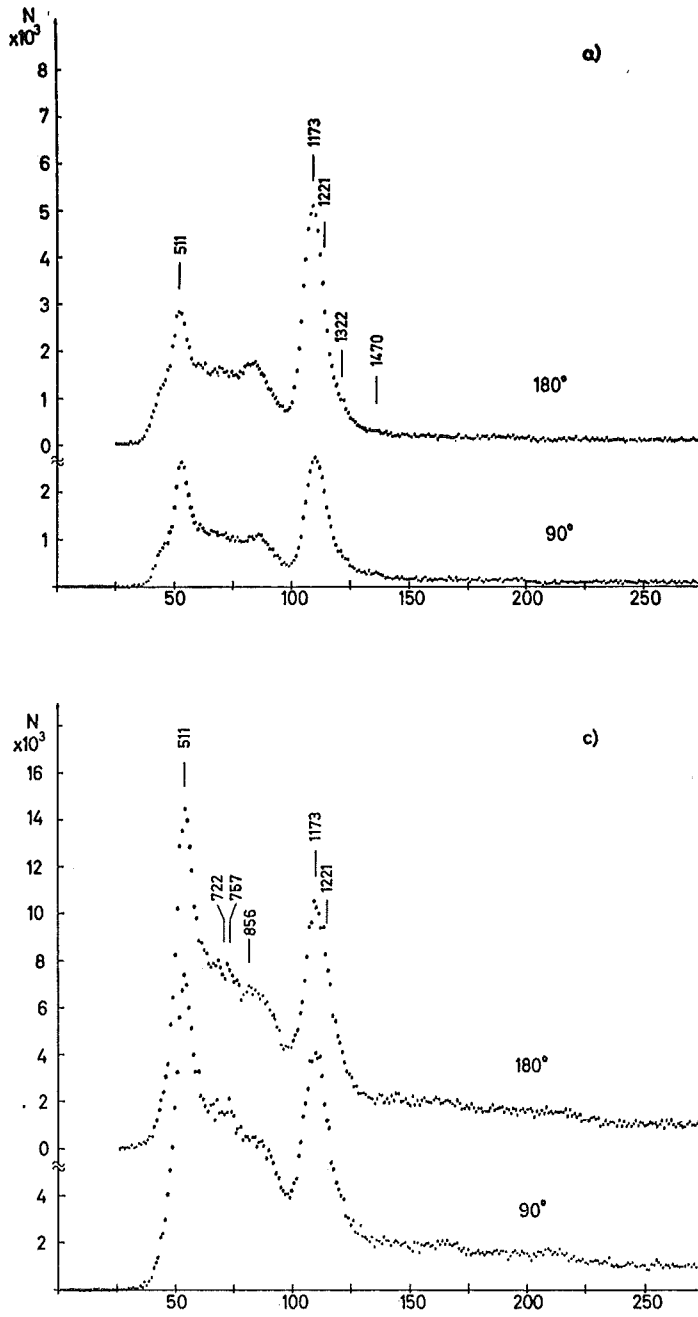


Fig. 4. NaI(Tl) spectra relevant to the angular correlation measurements. a-c) Spectra handled by the double window technique in coincidence with lines at 876 keV, 1173 keV and 2301/2346 keV. The 180° and 90° spectra are separated by shifting the ordinates.

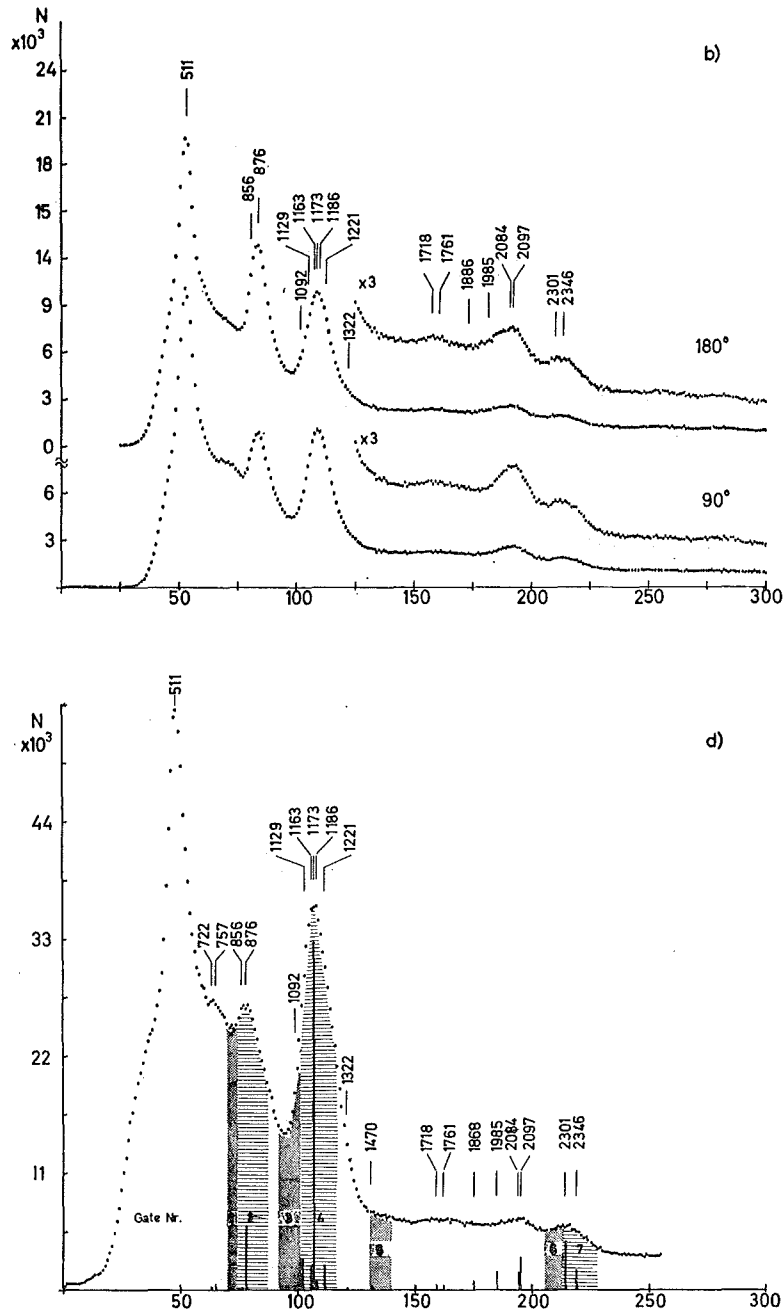


Fig. 4d. Singles spectrum taken with the stationary detector, showing the gates selected for the angular correlation measurements. The bars indicate the positions and intensities of prominent  $\gamma$ -rays as determined with the Ge(Li) anti-Compton spectrometer.

TABLE 8  
Results of angular correlation measurements; spin and multipole mixture determinations

Cascades <sup>a)</sup> (keV)	Corrected correlation coefficients <sup>b)</sup>		Spin sequence	Level spins		Multipole mixing			
	$A_2$	$A_4$		level energy (keV)	$J$	transition (keV)			
<u>876-1173</u>	+0.365±0.014	+1.139±0.020	0-2-0	2048	0	876	pure E2		
<u>1129-1173</u>	-0.070±0.015 <sup>c)</sup>	+0.069±0.027 <sup>c)</sup>	2-2-0	2301	2	1129	> 50 % E2		
<u>1163-1173</u>			4-2-0	2336	4	1163	pure E2		
<u>1186-(1163)-1173</u>			2, 3-4-2-0	3523	{2	1186	pure E2 <sup>d)</sup>		
<u>1186-1163</u>			2, 3-4-2			{3	1186		
<u>1221-(876)-1173</u>			-0.070±0.015 <sup>c)</sup>	+0.069±0.027 <sup>c)</sup>	1, 2-0-2-2	3270	{1	1221	pure M1 <sup>d)</sup>
<u>1221*-(1129)-1173</u>					2, 3-2-2-0	3523	{2	1221*	pure E2 <sup>d)</sup>
<u>1221*-1129</u>					2, 3-2-2			{3	1221*
<u>1718-1173</u>					+0.110±0.080	+0.280±0.120	2-2-0	2891	2
<u>1886-1173</u>			-0.180±0.070	+0.100±0.100	2-2-0	3059	2	1886	$\delta = -0.65^{+0.15}_{-0.20}$ <sup>e)</sup>
<u>1985-1173</u>			+0.150±0.060	+0.060±0.080	2-2-0	3158	2	1985	$\delta = -0.13 \pm 0.08$ <sup>e)</sup>
<u>2084-1173</u>	-0.154±0.024 <sup>c)</sup>	+0.028±0.043 <sup>c)</sup>	1, 2, 3-2-0	3257	1, 2, 3	2084			
<u>2097-1173</u>			1, 2-2-0	3270	1, 2	2097			
<u>2346-1173</u>	-0.140±0.030 <sup>c)</sup>	+0.143±0.056 <sup>c)</sup>	2-2-0	3518	2	2346			
<u>1221*-2301</u>									
<u>2346-1173</u>			-0.070±0.050	+0.11 ±0.070	2-2-0	3518	2	2346	$\delta = -0.44 \pm 0.09$ <sup>e)</sup>
<u>1221*-2301</u>	-0.050±0.060	+0.220±0.140	2-2-0	3523	2(?)	1221*	99 % E2(?)		
<u>2799-1173</u>	+0.380±0.150	+0.100±0.200	2-2-0	3972	2	2799			

<sup>a)</sup> Gates positioned at the underlined  $\gamma$ -rays.

<sup>b)</sup> The correlation coefficients in the expression  $W(\vartheta) = 1 + A_2 P_2(\cos \vartheta) + A_4 P_4(\cos \vartheta)$  obtained from the least-squares fit to the experimental data are corrected for target length and detector solid angle. Contributions of interfering cascades are estimated on the basis of the relative intensities listed in table 2.

<sup>c)</sup> Coefficient measured for the combined correlations of the contributing cascades.

<sup>d)</sup> Alternative interpretations presuming the spin values specified in column 6.

<sup>e)</sup> The interval of  $\delta$  has been determined from the uncertainty in  $A_2$ .

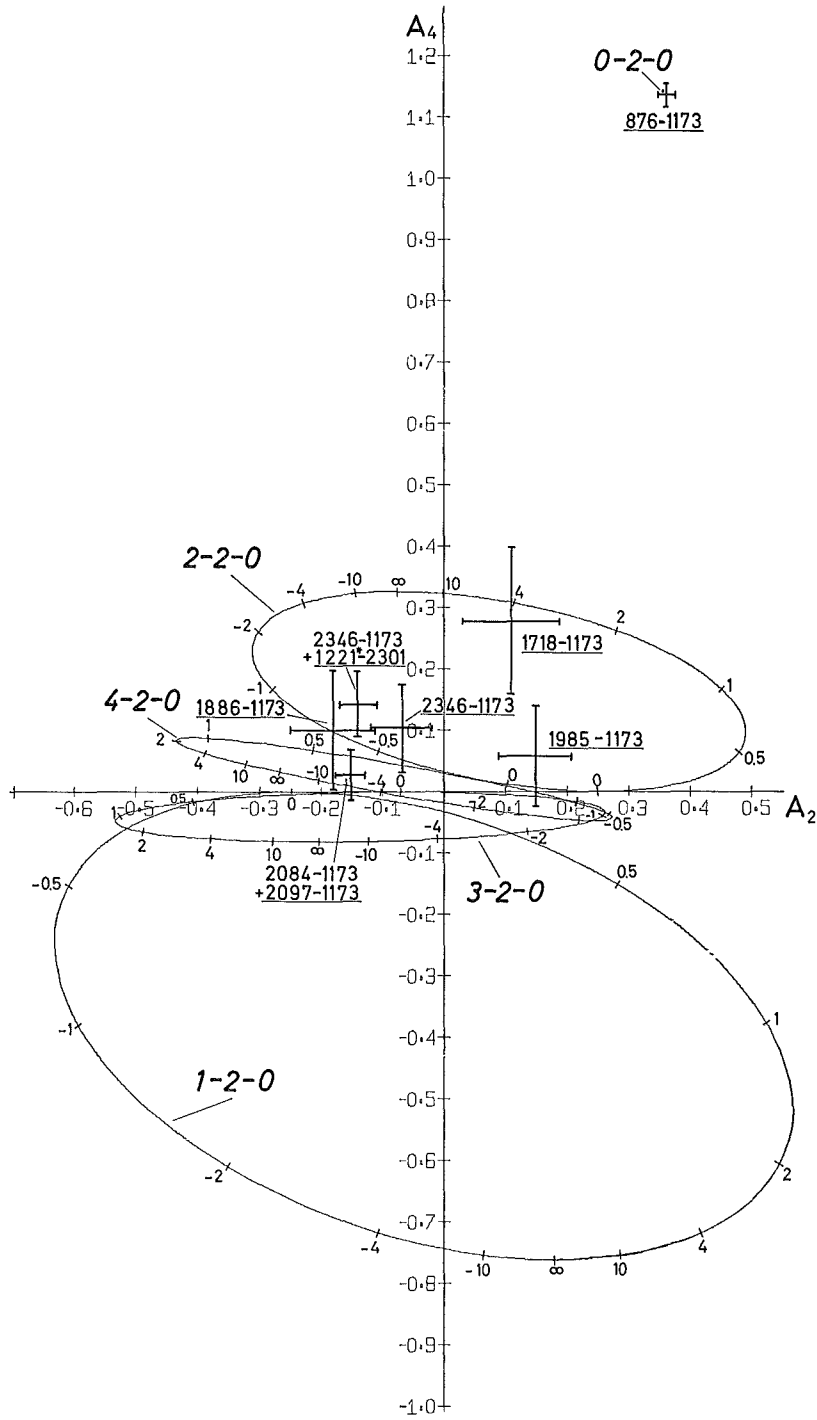


Fig. 5. Parametric representation of the  $A_2$  and  $A_4$  correlation coefficients for  $J-2-0$  cascades ( $J = 1, 2, 3, 4$ ). The corrected experimental values are plotted as crosses of error bars. As to the individual cascades see comments in the text.

decay scheme. The results are summarized in table 8 together with conclusions that are made as to spins and multipole mixing ratios. The measured coefficients are compared with the theoretical values on an  $A_2$ - $A_4$  plot in fig. 5.

Since the spin of the 2048 keV level is known from previous measurements<sup>8)</sup> to be zero, the angular correlation of the 876-1173 keV cascade was mainly used as a check of the performance of the apparatus and the data analysis. The perturbing contribution of the 856-(1129)-1173 keV cascade is less than 1.5%. Interference from the isotropic 1221-(876)-1173 keV triple cascade was either eliminated by a decomposition of the complex peak at 1173 keV in the spectrum coincident with the 876 keV line or by taking into account its contribution in coincidence with the window at 1.17 MeV. The excellent agreement of the observed coefficients with the theoretical coefficients for the 0-2-0 spin sequence  $A_2 = 0.358$  and  $A_4 = 1.142$  shows that the angular correlations of cascades proceeding through the 1173 keV level are practically not attenuated by extra nuclear fields<sup>†</sup>.

The multipole mixing of the 1129 keV transition is of great interest from a theoretical point of view. Unfortunately, the angular correlation of the 1129-1173 keV cascade is obscured by the correlations of several other cascades which have comparable intensities. The interfering cascades (keV) are the following (probable spin sequences<sup>††</sup> in brackets): 1129-1173 (2-2-0), 1163-1173 (4-2-0), 1186-(1163)-1173 (2- or 3-4-2-0), 1186-1163 (2- or 3-4-2), 1221-(876)-1173 (1- or 2-0-2-0), 1221\*-(1129)-1173 (2- or 3-2-2-0), 1221\*-1129 (2- or 3-2-2). It was estimated from the intensity values, the window position and the decay scheme that these seven cascades contribute to the observed angular correlation of the composite peak roughly in the proportion 10.2 : 11.6 : 5.0 : 5.0 : 4.2 : 2.5 : 1.8, respectively. The correlations of some of the cascades are known. But since there remain four unknown quantities, i.e. the spin of the 3523 keV level (2 or 3) and the multipole mixing ratios of the 1129 keV, the 1221\* keV, and the 1186 keV transition, it is not possible to derive the multipole mixing of the 1129 keV transition unambiguously from this measurement. Therefore, only rough estimates are given in the table. Two alternative solutions were obtained from the following considerations: (i) The analysis is based on the intensity proportion quoted above. Then meaningful values for the mixing parameter  $\delta$  of the 1129 keV transition can be derived from the observed correlation only with a spin  $J = 3$  assignment to the 3523 keV level. (ii) Major changes in the intensity proportions within the limits of errors (see table 2) are tolerated. Strictly speaking, these are justified only for the intensity ratio of the 1221\* keV and 1221 keV transition. Then the spin 2 assignment for the 3523 keV level cannot be excluded. Independent of the spin assignment to the 3523 keV level the analysis yields an E2 content of more than 50% for the 1129 keV transition. In the calculations the un-

<sup>†</sup> The half-life of the 1173 keV level is 2.0 psec [ref. <sup>32</sup>].

<sup>††</sup> The spin 4 assignment for the 2336 keV level is taken from ref. <sup>8</sup>). For the higher doublet level at 3523 keV spins lower than  $J = 2$  or spins higher than  $J = 3$  may be excluded because of the deexcitation to a  $4^+$  level and the presence of a primary transition from the  $1^-$ ,  $2^-$  capture state, respectively.

certainties of the experimental correlation coefficients have been taken into account. The result is consistent with the theoretical expectation.

The spin of the 2891 keV level which is involved in the 1718–1173 keV cascade is also of considerable theoretical interest. In evaluating the experimental correlation, interferences from the 1761–(1129)–1173 keV and from the 1985–1173 keV cascade have to be considered. The latter one affects the 1718–1173 keV correlation by the Compton edge of the 1985 keV transition. In addition, summing of the 1173 keV and neighbouring lines with the 511 keV annihilation radiation has to be taken into account. There are in total 12 cascades which give rise to sum peaks centered around 1.7 MeV. These peaks add up to an appreciable intensity which was estimated to be about  $\frac{1}{3}$  of the intensity of the 1718 keV  $\gamma$ -ray. It is clear that the summing effect introduces considerable uncertainty in the correlation coefficients. Nevertheless, the data seem to be sufficiently accurate to assign the spin 2 to the 2891 keV level. For the multipole mixing ratio of the 1718 keV transition then the value  $\delta = 4.1$  is obtained, i.e., this transition is of almost pure E2 character.

The 1886–1173 keV correlation is obscured by the presence of the Compton distribution of the strong 2.09 MeV peak the maximum of which is at about 1.83 MeV. The 2.09 MeV peak shows a relatively weak anisotropy (cf. below). If the 1886–1173 keV cascade would exhibit a very strong correlation as is to be expected for a 0–2–0 spin sequence it should have been recognized. This was not the case. Therefore, the spin 0 for the 3059 keV level was ruled out. The spin 2 assignment derived from the decay properties of this level is not in contradiction with the data obtained from the angular correlation measurements. It was then concluded from the positive level parity that the 1886 keV transition is an E2/M1 mixture with an E2 content of probably less than 40 %.

The 1985 keV transition is a component of the complex peak at 2.09 MeV in the spectrum coincident with the 1173 keV line (see fig. 4b). The decomposition of this composite group with the above mentioned computer program gave rise to larger uncertainties in the intensities of the 1985 keV line and, as a consequence, in the angular correlation coefficients of the 1985–1173 keV cascade, especially in the  $A_4$  coefficient. From the experimental data available most probably the spin-parity  $J^\pi = 2^+$  has to be assigned to the 3158 keV level. The spins 3 and 4 are excluded on the basis of the deexcitation mechanism of this level. There is probably only a small E2 admixture in the 1985 keV transition.

A decomposition of the 2084 keV and the 2097 keV  $\gamma$ -lines was not possible. Therefore, the correlation coefficients given in the table refer to the combined angular correlations of the 2084–1173 keV and the 2097–1173 keV cascade. Owing to the uncertainties in the  $A_4$  coefficient, no definitive conclusions on the spins of the 3257 keV and the 3270 keV level can be drawn from these measurements without further assumptions. If, e.g.,  $A_4 = 0$  is assumed, the assignment of the spin 3 for the 3257 keV level and of the spin 1 for the 3270 keV level is unambiguous. This follows from a consideration of the contributions of the two cascades to the observed correlation

( $I_{2084}/I_{2097} = 4.0/7.2$ ). The parities of the levels are known to be positive. The 2084 keV and the 2097 keV transitions are then both of pure M1 character. A measurement of the internal conversion coefficients would be of particular interest in this case.

Since the window at 1173 keV covers also the 1221 keV  $\gamma$ -line, the peak at 2.3 MeV in the coincidence spectrum consists of the 2301 keV and the 2346 keV transition. This is clear from an inspection of the decay scheme showing that the 2301 keV  $\gamma$ -line must appear as a member of the 1221\*-2301 keV cascade. Again, the 2301 keV and the 2346 keV transition cannot be resolved and the observed angular correlation is the sum of the individual correlations of the 2346-1173 keV and the 1221\*-2301 keV cascade. The contribution of the last one is only approximately known, since the intensity of the 1221\* keV transition is uncertain. Interference from the 2799-1173 keV cascade via the single escape peak of the 2799 keV  $\gamma$ -ray is negligible. The measurement is consistent only with a spin 2 or 4 assignment to the 3518 keV level. This assignment is independent of the spin (2 or 3) of the 3523 keV level and the multipolarity of the 1221\* keV transition because of the relatively small contribution of the 1221\*-2301 keV cascade. Since the 3518 keV level is deexcited by the 1470 keV  $\gamma$ -ray to the  $0^+$  level at 2048 keV, the spin 4 is ruled out. The multipole mixture of the 2346 keV transition cannot be determined with confidence due to the lack of information on the 1221\*-2301 keV cascade. Because of the positive parity of the 3518 keV level it is assumed, that the multipolarity of the 2346 keV transition is an E2/M1 mixture. Most probably the E2 admixture is less than 30 %. A similar situation as above is observed with the gate at 2.3 MeV covering both the 2301 MeV and the 2346 keV transition. By decomposing the complex peak at 1173 keV in the coincidence spectrum (see fig. 4c) into the components, the 1173 keV and the 1221\* keV  $\gamma$ -line, it was possible to extract the individual correlations of the 2346-1173 keV and the 1221\*-2301 keV cascade. The resulting correlation coefficients for the 2346-1173 keV cascade are only in fair agreement with the former values showing that there must be other interferences which have not been taken into account. Possibly there is a contribution of the 1092-(757)-2301 keV cascade. This contribution is difficult to estimate since nothing is known about the correlation of that cascade. The spin 2 assignment to the 3518 keV level, however, remains unaffected. The results for the 1221\*-2301 keV cascade point at a spin 2 assignment for the 3523 keV and an almost pure E2 character of the 1221\* keV transition. This result has to be compared with the analysis of the complex peak at 1173 keV in the spectrum coincident with the window at 1173 keV. Consistency as to the spin assignment is only achieved if the intensity proportions of the various cascades involved in that analysis are varied as assumed in (ii). In this case, however, the analysis of the complex 1.17-1.17 MeV correlation suggests smaller values for the mixing parameter of the 1221\* keV transition. Because of the greater statistical errors and the uncertainty introduced by the unfolding procedure of the 1173 keV peak the 1221\*-2301 keV correlation is believed to be less confident.

The existence of the relatively strong 3972 keV transition proceeding from the 3972 keV level to the ground state excludes the spin 0 and spin values higher than 2

for this level. Thus for the 2799–1173 keV cascade there are only two alternative spin sequences (1–2–0 and 2–2–0). Although the total absorption peak of the 2799 keV  $\gamma$ -ray is not very pronounced the data obtained for the 2799–1173 keV correlation are statistically significant to rule out the spin 1 for the 3972 keV level. The multipolarity of the 2799 keV transition cannot be determined from this measurement.

#### 4. Discussion

There is a high degree of agreement between the  $(n, \gamma)$  levels and those found in other investigations, if small energy deviations – due to the poorer energy accuracy in previous measurements – are neglected. For excitation energies higher than 4 MeV the comparison gets difficult due to the increasing level density, and the  $(n, \gamma)$  scheme is certainly not complete in that region. Up to 4 MeV only two levels are missing in the  $(n, \gamma)$  scheme compared with the results of most of the other measurements: the levels at 3175 keV and 3467 keV. Probably one has to assign the spins  $J = 4, 5$  to these states, consistent with the  $l_n = 3$  transfer in the  $(d, p)$  reaction<sup>8)</sup>. From the  $\beta$ -decay data<sup>9)</sup> of  $^{62}\text{Co}$  the spin  $J = 4$  for the state at 3175 keV is more probable.

One previously known level at 3.52 MeV has been resolved as a doublet with a level spacing of 4 keV in the  $(n, \gamma)$  reaction. Strong arguments for the introduction of this doublet are the well-established coincidences 2346–1173 keV and 1221\*–2301 keV and the doublet character of the 7077 keV line (cf. fig. 1) interpreted as a primary transition. One consequence is that the line at 1220.76 keV (cf. table 2) has to be considered a doublet. From the line shape the spacing was estimated to be less than 400 eV. As mentioned in subsect. 3.4, the angular correlation of the 2346–1173 keV cascade as well as feeding and deexcitation of the lower doublet level at 3518 keV are consistent with  $J^\pi = 2^+$ . From the decay properties of the higher doublet level at 3523 keV spins other than  $J = 2$  or  $J = 3$  have to be excluded. The deexcitation of the level (doublet) at 3.52 MeV by a 1220 keV transition to the state at 2301 keV was also observed by Beuzit *et al.*<sup>11)</sup>.

From cross sections and angular distributions in inelastic scattering experiments<sup>8)</sup> with protons,  $^3\text{He}$  and  $\alpha$ -particles there is evidence for a collective  $3^-$  state in the excitation-energy region 3.70 MeV to 3.80 MeV. In the compilation of ref.<sup>8)</sup> this state has been identified with a  $(d, p)$  level at 3751 keV for which an angular-momentum transfer of  $l_n = 1$  and 3 has been measured. Obviously, this interpretation is not compatible in parity, but justified somehow by the fact that other experiments, too, find only one level between 3.70 MeV and 3.80 MeV. Therefore, the  $(n, \gamma)$  level constructed at 3757 keV is thought to be that first octupole-phonon  $3^-$  state. This  $3^-$  level could be fed directly by an M1 transition of 6839 keV from the capturing state. The existence of such a (weak) transition cannot be established because of the appearance of a strong  $^{63}\text{Ni}$  line at 6840 keV in the  $(n, \gamma)$  spectrum (see fig. 1). The character of deexcitation of the 3757 keV level is confirmed by  $(p, p'\gamma)$  studies of Beuzit<sup>11)</sup>.

One particularly interesting state in  $^{62}\text{Ni}$  is the level at 2.89 MeV. Its existence now

seems to be well established by various reactions. It has also been discussed in connection with the  $^{62}\text{Co}$  decay. Way *et al.* introduced a  $^{62}\text{Ni}$  level at 2.89 MeV (fig. 6b) by changing the sequence of two  $\gamma$ -transitions, 1.74 MeV and 1.47 MeV, in the early  $^{62}\text{Co}$  decay scheme proposed by Gardner *et al.* [cf. ref.<sup>9</sup>] and see fig. 6a],

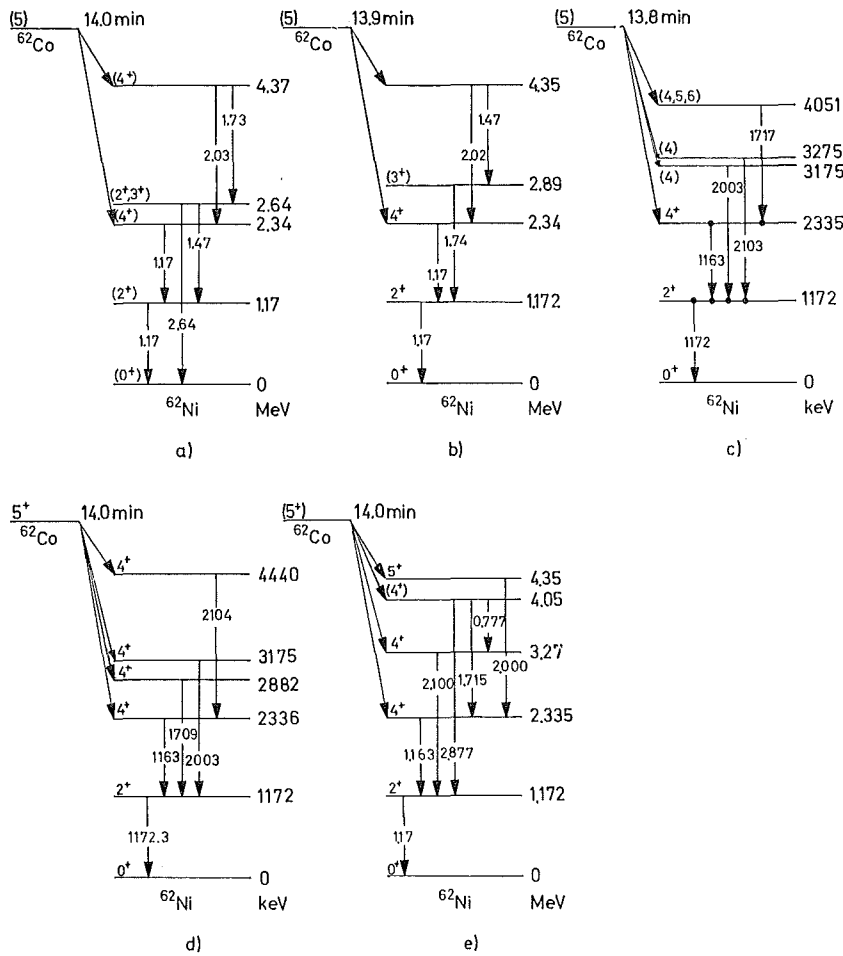


Fig. 6. Decay schemes of  $^{62}\text{Co}$  a) as proposed by Gardner and Meinke [cf. ref.<sup>9</sup>]; b) as given by Way *et al.* [cf. ref.<sup>9</sup>]; c) as proposed by Mo *et al.*<sup>9</sup>); d) as proposed by Kiselev *et al.*<sup>33</sup>); e) as proposed by Ward *et al.*<sup>34</sup>).

in order to reconcile the data with nuclear reaction results. Although the deexcitation of a 2.89 MeV level by a 1.74 MeV  $\gamma$ -ray would agree with the  $(n, \gamma)$  transition diagram, Way's modification seems to be doubtful. The decay measurements were recently repeated by Mo *et al.*<sup>9</sup>), using Ge(Li) diodes for the detection of  $\gamma$ -rays. The  $\beta$ -spectrum was not investigated by these authors. The result is presented in

fig. 6c. Mo *et al.* found the lines 1163 keV and 1717 keV (corresponding to the earlier 1.74 MeV  $\gamma$ -ray) to be coincident. Since the 1163 keV line is a well-established transition between the levels at 2.33 MeV and 1.17 MeV, they concluded that the 1717 keV  $\gamma$ -ray feeds the state at 2.33 MeV and that, consequently, the 2.89 MeV level is not fed in the 14 min decay of  $^{62}\text{Co}$ . If this interpretation is correct, the agreement in the energy of the  $\gamma$ -rays at 1717 keV found in the  $^{62}\text{Co}$  decay and in the  $(n, \gamma)$  reaction has to be considered as fortuitous. Two further proposals<sup>†</sup> for the 14 min decay of  $^{62}\text{Co}$  shown in the figs. 6d and e still do not clarify the situation. In the scheme of Kiselev *et al.*<sup>33)</sup> Way's version of a 1.74 MeV transition depopulating the 2.89 MeV level seems to be confirmed. A spin  $J = 4$  assignment for this state is in contradiction to our measurements. In the proposal of Ward *et al.*<sup>34)</sup> some similarity to Mo's diagram may be seen. No information<sup>††</sup> on the possible population of the 2.89 MeV state in the decay of  $^{62}\text{Cu}$  is given in the literature up to now, although this decay was reinvestigated recently by Jongsma *et al.*<sup>10)</sup>. In a latest publication on  $(p, t)$  reaction measurements<sup>35)</sup> a  $0^+$  state at 2.85 MeV in  $^{62}\text{Ni}$  is reported. Supposed, this level in a well-known excitation-energy region is not absolutely new, one has to identify it with the 2.89 MeV state. The  $0^+$  assignment could help to understand why no  $\gamma$ -ray transitions to the  $0^+$  ground state and the second excited state with  $J = 0$  were observed; but it is excluded in the analysis of  $\gamma$ - $\gamma$  angular correlations.

Nine recoil corrected primary transitions and their corresponding level energies, as determined from the low-energy  $\gamma$ -ray data, have been used for calculating the binding energy  $B_n$  of the last neutron in the nucleus  $^{62}\text{Ni}$ . The weighted mean value is

$$B_n = 10596.2 \pm 1.5 \text{ keV.}$$

The uncertainty includes systematic errors from the calibration  $\gamma$ -lines. The previously known<sup>36)</sup>  $B_n$  values from mass spectrometry and  $Q$ -values of  $(d, p)$  measurements were  $10599 \pm 6$  keV and  $10604 \pm 8$  keV.

Since the  $(n, \gamma)$  investigation yields a lot of new information on transition modes and level spins, it is stimulating to compare the data with the results of recent shell-model calculations. Fig. 7 presents the experimental levels (including two states from other investigations) and four theoretical schemes<sup>4-7)</sup>. The common assumptions of the calculations have been summarized in sect. 1. In the right-hand level scheme surface delta interaction<sup>5)</sup> was applied with an attractive strength constant fitted to the odd-even mass difference. The agreement of the low-lying levels with experiment is surprisingly good. In the scheme of Hsu<sup>4)</sup> the nucleon-nucleon potential used was an s-state interaction with four radial matrix elements, as suggested by a least-squares fit to 27 experimental Ni energy values. In refined calculations Cohen *et al.*<sup>6)</sup> parametrized a two-body potential with central, tensor and two-body spin-orbit

<sup>†</sup> These two works have come to our knowledge during completion of this publication.

<sup>††</sup> Upon completion of this work we have been informed on a new investigation of the  $^{62}\text{Cu}$  decay performed by Van Patter *et al.* The decay scheme is quite consistent with the  $(n, \gamma)$  transition diagram, also with respect to the deexcitation of the 2.59 MeV level.

parts together with the four radial matrix elements. This procedure yields 8 free parameters to be fitted to 24 experimental level energies in different nickel isotopes. Finally Auerbach <sup>7)</sup> fitted 17 of a total of 30 matrix elements to the body of available energy data, using the Kallio-Kolltveit potential for calculating the rest of them. On the whole the agreement is not bad in the low-energy region up to 3.2 MeV.

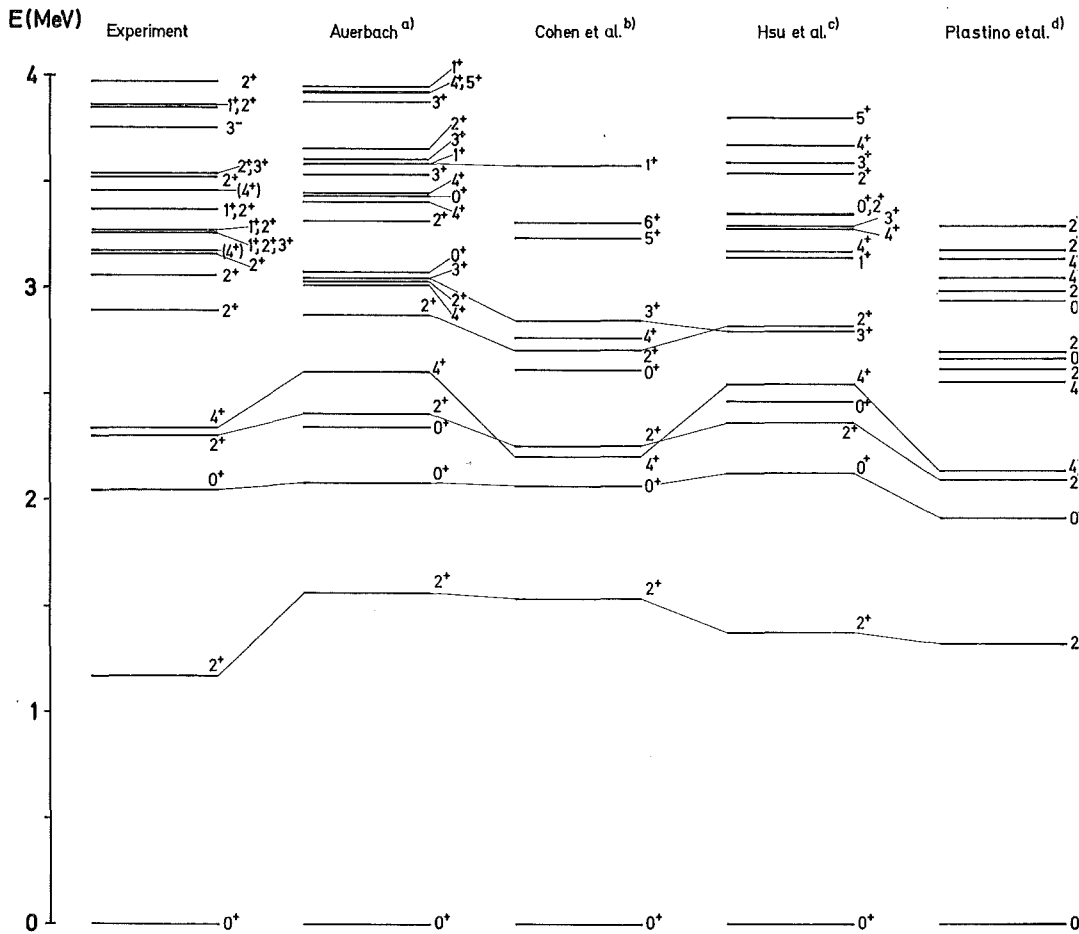


Fig. 7. Comparison of the experimental level scheme with results of exact shell-model calculations. a) Ref. 7). b) Ref. 6). c) Ref. 4). d) Ref. 5).

Above this limit there appear some high-spin states in Cohen's and Hsu's schemes, for which there is no experimental evidence up to now. It is not yet possible to define the exact position of the first  $3^+$  level; but the theoretical predictions seem to be a little too low in any case. It is strange that in all experiments <sup>†</sup> no further  $0^+$  states were observed than the one at 2.05 MeV. Levels with  $J^\pi = 0^+$  should be fed strongly

<sup>†</sup> One exception is the spin 0 assignment for a level at 2.85 MeV in ref. <sup>35)</sup> which has been discussed above.

in the  $(n, \gamma)$  reaction. Therefore the theoretical predictions of several  $0^+$  states beyond 2.05 MeV are in contradiction to the hitherto known experimental observation. The experimental  $3^-$  state, of course, cannot be reproduced within the configurations chosen.

Much more sensitive to the interactions used in the calculations are the reduced transition probabilities rather than the level positions. Of particular interest is the ratio  $b = B(E2; 2_2^+ \rightarrow 2_1^+)/B(E2; 2_2^+ \rightarrow 0_1^+)$ . Due to a wrong spin assignment the first experimental  $b$ -value<sup>37)</sup> cited several times in the literature was  $b < 210$ . Recent measurements of the  $^{62}\text{Cu}$  decay<sup>10)</sup> and the  $(p, p'\gamma)$  reaction<sup>11)</sup> yielded  $b < 14 \pm 7$  and  $b < 35^\dagger$ , respectively. The values represent upper limits only since pure E2 radiation was assumed. For comparison, the upper limit of this investigation is  $b < 23 \pm 4$ , if the same assumption is made. Regarding the measured E2 content of more than 50 % in the 1129 keV transition we arrive at  $11 < b < 23$ . The theoretical values of Cohen and Auerbach are  $b = 33$  and  $b = 1310$ , respectively. The agreement with the prediction of Cohen's shell-model calculation has to be considered as quite satisfactory. From the branching ratios compiled in table 7 one may calculate some more limits for ratios of reduced transition probabilities, but there is a lack of theoretical predictions. It would be of great interest to extend this comparison with theory to higher-excitation states.

<sup>†</sup> Calculated from the intensity ratio 50 : 50 reported in ref. <sup>11)</sup>.

### References

- 1) A. K. Kerman and C. M. Shakin, Phys. Lett. **1** (1962) 151
- 2) H. W. Broek, Phys. Rev. **130** (1963) 1914
- 3) R. K. Mohindra and D. M. Van Patter, Phys. Rev. **139** (1965) B274
- 4) L. S. Hsu and J. B. French, Phys. Lett. **19** (1965) 135;  
L. S. Hsu, Nucl. Phys. **A96** (1967) 624
- 5) A. Plastino, R. Arvieu and S. A. Moszkowski, Phys. Rev. **145** (1966) 837
- 6) S. Cohen, R. D. Lawson, M. H. Macfarlane, S. P. Pandya and M. Soga, Phys. Rev. **160** (1967) 903
- 7) N. Auerbach, Phys. Rev. **163** (1967) 1203
- 8) H. Verheul, Nucl. Data **B2** (Oct. 1967) 1
- 9) J. N. Mo, S. Ray and S. K. Mark, Nucl. Phys. **A125** (1969) 440
- 10) H. W. Jongsma, B. Bengtsson, G. H. Dulfer and H. Verheul, Physica **42** (1969) 303
- 11) P. Beuzit, J. Delaunay and J. P. Fouan, Nucl. Phys. **A128** (1969) 594
- 12) U. Fanger, G. Markus, W. Michaelis, H. Ottmar and H. Schmidt, KFK 616 (1967)
- 13) W. Michaelis, private communication (1967) to Nucl. Data **B2-3-1** (1967);  
U. Fanger, G. Markus, W. Michaelis, H. Ottmar and H. Schmidt, Proc. Int. Conf. on nuclear structure, Tokyo (1967) p. 152
- 14) U. Fanger, R. Gaeta, W. Michaelis, H. Ottmar and H. Schmidt, Neutron capture  $\gamma$ -ray spectroscopy, IAEA, Vienna, 1969, 273
- 15) U. Fanger, W. Michaelis, H. Schmidt and H. Ottmar, Nucl. Phys. **A128** (1969) 641
- 16) L. V. Groshev, A. M. Demidov and N. Shadiev, Sov. J. Nucl. Phys. **3** (1966) 444
- 17) Nuklidkarte, 3rd edition, Kernforschungszentrum Karlsruhe, Gersbach, München 1968
- 18) W. Michaelis and H. Küpfer, Nucl. Instr. **56** (1967) 181
- 19) G. Markus, thesis, University of Karlsruhe

- 20) U. Fanger, KFK 887 (1969)
- 21) H. Schmidt, KFK 877 (1969)
- 22) G. Krüger, G. Dimmler, G. Zipf, H. Hanak and R. Merkel, *Kerntechnik* **8** (1966) 273
- 23) J. Legrand, J. P. Boulanger and J. P. Brethon, *Nucl. Phys.* **A107** (1968) 177
- 24) R. L. Graham, G. T. Ewan and J. S. Geiger, *Nucl. Instr.* **9** (1960) 245
- 25) G. Murray, R. L. Graham and J. S. Geiger, *Nucl. Phys.* **63** (1965) 353
- 26) W. W. Black and R. L. Heath, *Nucl. Phys.* **A90** (1967) 650
- 27) H. E. Jackson, A. I. Namenson and G. E. Thomas, *Phys. Lett.* **17** (1965) 324
- 28) R. K. Shelton and W. N. Shelton, H. T. Motz and R. E. Carter, *Phys. Rev.* **136** (1964) 351
- 29) R. C. Greenwood, private communication to *Nucl. Data* **A4** (1968) 316
- 30) V. Haase, KFK 730 (1968)
- 31) W. Michaelis, KFK 135 (1963)
- 32) P. H. Stelson and L. Grodzins, *Nucl. Data* **A1** (1965) 21
- 33) B. G. Kiselev, V. N. Levkovskii and I. V. Kazachevskii, *Yad. Fiz.* **8** (1968) 1063
- 34) T. E. Ward, P. H. Pile and P. K. Kuroda, *J. Inorg. Nucl. Chem.* **31** (1969) 3023
- 35) W. G. Davies *et al.*, Montreal Int. Conf. on properties of nuclear states (August 1969)
- 36) G. A. Bartholomew *et al.*, *Nucl. Data* **A3**, 4-6 (1967) 377
- 37) D. M. Van Patter, *Nucl. Phys.* **14** (1959-1960) 42